A Theory for the Indian Ocean Dipole Mode

Tim Li, Bin Wang, C.-P. Chang*, and Yongsheng Zhang

International Pacific Research Center, University of Hawaii, Honolulu, Hawaii

*Department of Meteorology, Naval Postgraduate School, Monterey, California

(Submitted to J. Atmos. Sci., June 7, 2002)

Corresponding Author: Prof. Tim Li, IPRC and Department of Meteorology, University of Hawaii, 2525 Correa Rd., Honolulu, HI 96822. E-mail: **timli@hawaii.edu**

Abstract

A conceptual coupled atmosphere-ocean model was constructed to understand the origin of the Indian Ocean Dipole Mode (IODM). In the model various positive and negative air-sea feedback processes were involved. Among them were the cloud-radiation-SST feedback, the evaporation-SST-wind feedback, the thermocline-SST feedback, and the monsoon-SST feedback. Numerical results indicate that air-sea interactions in the tropical Indian Ocean support a natural damped mode, which is different from the self-sustained ENSO mode in the tropical Pacific. The difference arises from the distinctive characteristics of the basic state of the coupled system in the tropical Indian and Pacific Oceans. By use of observational analyses and physical reasoning, the authors identified four fundamental differences between air-sea interactions in the two oceans. The first difference is represented by the strong contrast of the cloud-SST phase relationship between the warm pool and cool tongue. The second difference arises from the reversal of the basic-state zonal wind and east-west tilting of the ocean thermocline, which leads to distinctive effects of ocean waves on the SST. The third difference lies in the existence of the Asian monsoon and its negative feedback on the IODM. The fourth difference is that the southeast Indian Ocean is a region where there exists a positive atmosphere-ocean thermodynamic feedback.

The phase-locking of the IODM can be, to a large extent, explained by the seasonal dependence of the aforementioned thermodynamic air-sea feedback. In addition, anomalous Indian monsoon also plays a role. Although the El Nino exerts the strongest forcing toward the end of a year, its impact on the anomalous monsoon heating peaks in

northern summer. Thus the anomalous monsoon may exert the greatest impact on the IODM toward the end of boreal summer.

In the presence of realistic ENSO forcing, the model was capable of simulating most of IODM events during the last 50 years that were associated with ENSO, indicating that ENSO is one of major forcings that trigger the IODM events. The failure of simulation of the IODM events in 1961 and 1994 suggests that other types of climate forcing may also play a role. The authors' observational analyses revealed that the 1994 event resulted from anomalous heating over Indochina/South China Sea in boreal summer, whereas the 1961 event might be traced back to the preceding winter when there was anomalous heating over the maritime continent.

1. Introduction

This study is motivated by observational discovery that there is a remarkable SST dipole (or zonal) mode in the equatorial Indian Ocean (hereafter, IODM) and that this dipole SST mode might arise from dynamic atmosphere-ocean interactions in the Indian Ocean (IO) (Saji et al. 1999, Webster et al. 1999). Although the dipole structure has been known for a while, mostly with modest amplitudes (e.g., Reverdin et al. 1986), the IODM attracted great public attention in 1997 when it reached extremely high magnitude and was associated with severe floods in East Africa and droughts over Indonesia. It was suggested that the unusual Indian monsoon-ENSO relationship in 1997 might result from this abnormal SST condition in the IO (Ashok et al. 2001).

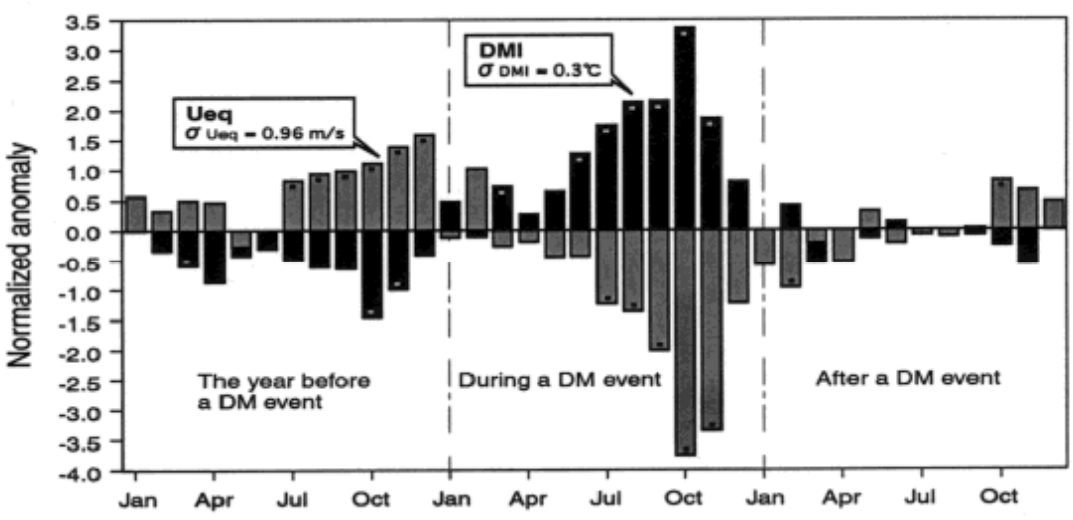

Fig. 1 Time evolution of the dipole mode index defined as the SSTA difference between the western and eastern Indian Ocean (dark shaded bar) and the zonal wind anomaly (light shaded bar), adopted from Saji et al. (1999).

Figure 1 shows the temporal evolution of composite SST and zonal wind anomalies associated with the IODM. The IODM develops rapidly in boreal summer and reaches its mature phase in October. Thus the first fundamental issue that requires the theoretical

understanding is why the phase of the IODM locks into the annual cycle. Similarly, one may ask why the mature phase of the IODM differs from that of ENSO, which has maximum amplitude in boreal winter. The second feature one may infer from Fig. 1 is that there is strong air-sea coupling over the IO, because of close wind-SST relationships. This prompts some investigators to hypothesize that the similar mechanism as that in ENSO might work in the IO. However, it is worth noting that the tropical Pacific and IO have remarkable differences in basic-state wind and SST fields. A theoretical study by Wang and Xie (1998) pointed out that ocean-atmosphere interactions are fundamentally different in warm and cold oceans. Thus the second issue we address is what are fundamental differences between air-sea interactions in the tropical Pacific and Indian Oceans. The third feature in Fig. 1 is that the IODM tends to have a biennial frequency, that is, the anomalous SST gradient changes the sign from one year to the following year. What is the physical mechanism responsible for this biennial tendency?

In this study we intend to answer these questions. The rest of this paper is organized as follows. In section 2, we analyze the fundamental differences between air-sea coupling processes in the tropical Pacific and Indian Oceans, based on observational analyses and physical reasoning. We note that air-sea interactions in the two oceans have four distinctive features. These distinctive features arise primarily from remarkable differences in the basic-state wind and SST fields. Based on these analyses, in section 3 we construct a conceptual air-sea coupled model for the IODM. We then discuss the solutions of the model in the presence of atmosphere-ocean interactions in section 4 and external ENSO and intraseasonal oscillation (ISO) forcing in section 5. In subsequent sections we further discuss the mechanisms related to the phase-locking and biennial periodicity, the effect of ocean waves, and the possible causes of 1994 and 1961 IODM events. A concluding remark is given in the last section.

2. Fundamental differences between air-sea interactions in the tropical Pacific and IO

To understand the origin of the IODM, one needs first to understand the similarities and differences of air-sea coupling processes in the equatorial Pacific and IO. In the following, by use of observational analyses and physical reasoning, we demonstrate that there are four major differences between the air-sea interactions in the tropical IO and Pacific.

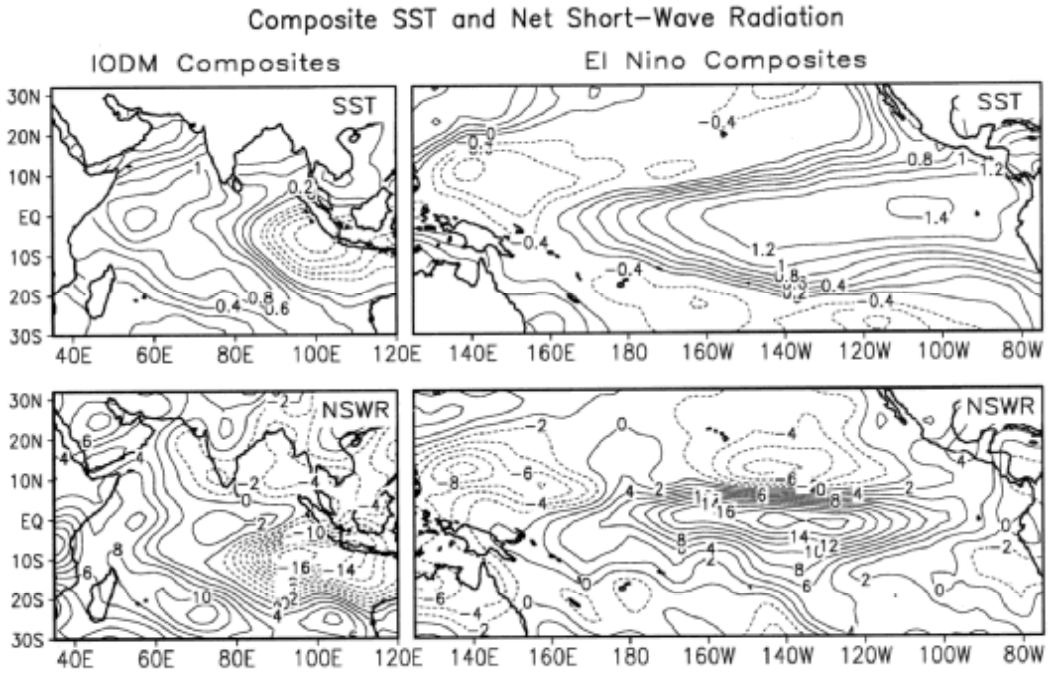

Fig. 2 Horizontal structure of SSTA (°C) and net shortwave radiation anomalies (Wm^{-2}) composed from 12 major El Nino and 6 IODM events during 1950-1999.

The first difference is the cloud-radiation-SST feedback. Figure 2 shows the observed SST and net surface shortwave radiation fields obtained from the El Nino and IODM composites for 1950-1998. [For the El Nino composite, 12 El Nino episodes were selected, whereas for the IODM composite, 6 dipole events were selected, following Saji et al. (1999).] A remarkable difference between the two composites is that the SST and shortwave radiation (or cloud) anomalies have significant zonal phase differences in the Pacific but not in the IO.

The differences arise from the distinctive atmospheric responses to a SST anomaly (SSTA) in the warm pool and cold tongue. In general, atmospheric deep convection is triggered in the region where SST is above 26.5°C. This is why anomalous convection associated with El Nino is often observed in the central equatorial Pacific even though the maximum SSTA appears in the eastern Pacific. Because of this phase difference, the reduction of the downward shortwave radiation due to the deep convection cannot efficiently damp the El Nino. In warm oceans, on the other hand, a modest SSTA may induce deep convection in situ, so that the anomalous SST and clouds are generally in phase. The increased clouds tend to reduce the downward shortwave radiation and thus decrease the SST, leading to a negative feedback between the atmosphere and ocean.

The strength of the cloud-radiation-SST feedback may be estimated in the warm ocean based on a linear Newtonian damping formula:

$$D_{SW}T = -\frac{Q_{SW}}{\rho c_w h} \quad ,$$

where D_{SW} is the Newtonian cooling coefficient representing the strength of the negative feedback, and *h* is the mean depth of the oceanic mixed layer. According to the composite SST-radiation relationship in the IO, the SSTA amplitude of 0.5°C corresponds to the net shortwave radiation anomaly of 10 Wm^{-2}. Thus for given a mixed layer depth of 50 m, one may calculate D_{SW}, which corresponds to a reversed damping time scale of 100 days. Such a strong damping implies that SST variability in warm oceans is in general small unless there is a strong positive air-sea feedback or persistent external forcing.

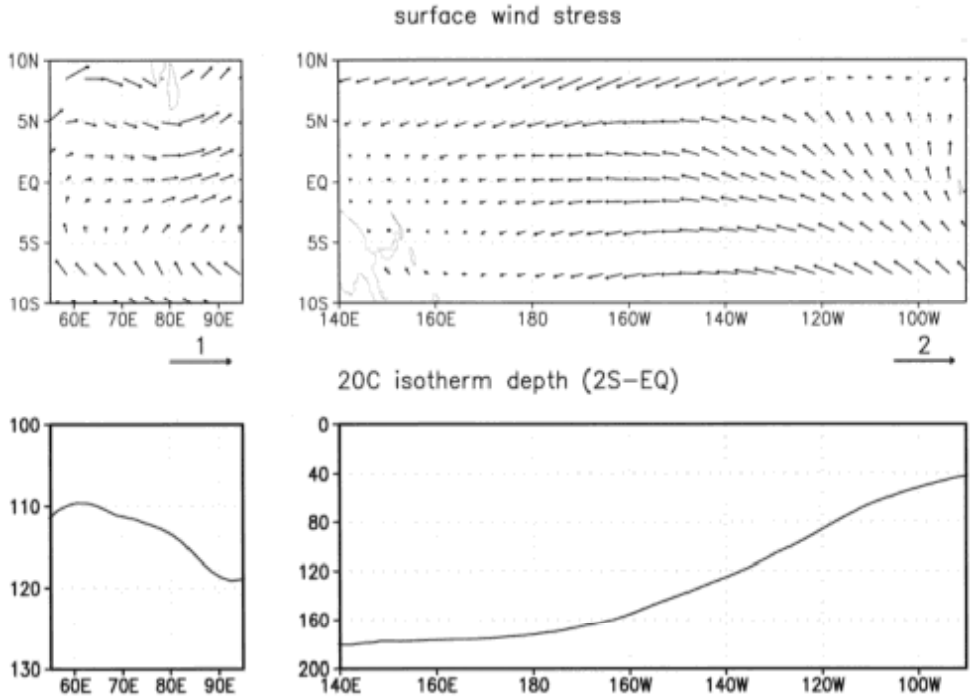

Fig. 3 Structure of observed annual mean surface wind stress (Nm^{-2}) fields and zonal distribution of the ocean 20°C isotherm depth (m) fields along the equatorial Pacific and Indian Ocean

The second difference is associated with basic-state winds and the effect of ocean waves. Whereas the tropical Pacific is dominated by easterly trades, the winds in the tropical IO are characterized by strong north-south monsoonal circulation. At the equator, the annual mean wind is strong easterly in the Pacific but weaker westerly in the IO. Such a difference results in opposite thermocline gradients across the two ocean basins (Fig. 3).

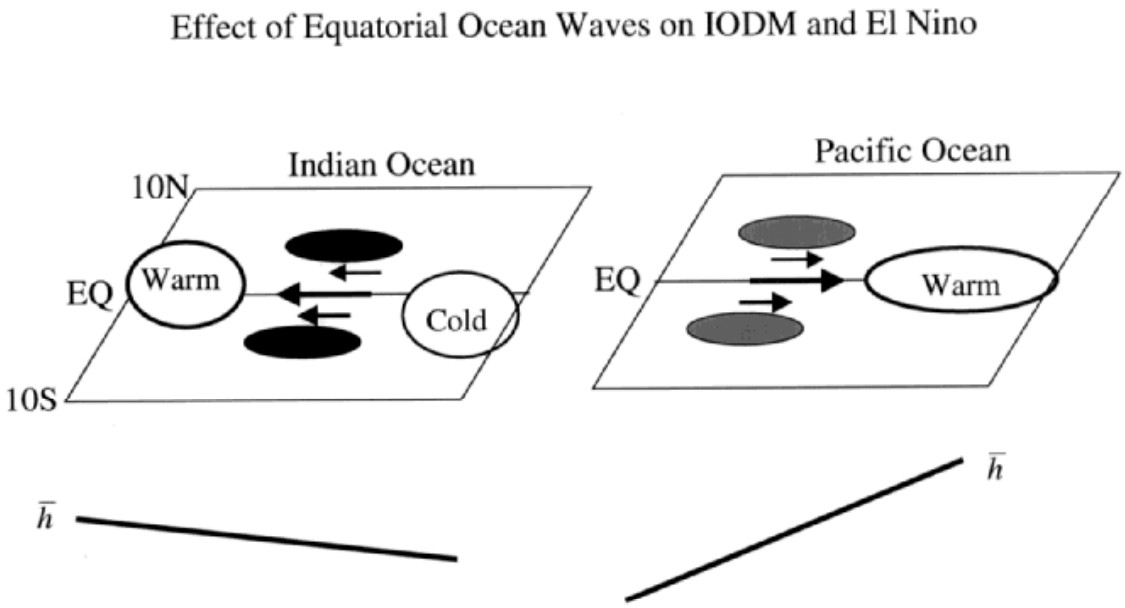

Fig. 4 Schematic diagram of effect of equatorial oceanic waves on the El Nino and the IODM. Dark (light) shaded regions represent positive (negative) ocean thermocline depth anomalies.

The reversal of the basic-state winds and zonal thermocline gradients in the IO implies that the effect of equatorial ocean waves could be significantly different from the Pacific counterpart. The schematic diagram of Fig. 4 illustrates how the wave effect can be different. In the Pacific, a warming in the eastern Pacific leads to westerly anomalies in the central Pacific that further induce off-equatorial Rossby waves with negative thermocline depth anomalies. After reflection in the western boundary, these Rossby waves become equatorial upwelling Kelvin waves and propagate eastward, reversing the sign of the SSTA later (Schopf and Suarez 1988, Battisti and Hirst 1989). Thus, in the El Nino scenario, ocean Rossby waves act as a negative feedback agent and are responsible for the phase reversal. In the IO, equatorial easterly

anomalies occur in response to a positive phase of the IODM[1]. The curl of the wind stress anomalies generates oceanic Rossby waves that carry deeper thermocline depth anomaly signals and propagate westward, enhancing the warm SSTA in the western IO where the mean thermocline is relatively shallow (Xie et al. 2002). The signals of the Rossby wave propagation and associated enhancement of the ocean surface warming were clearly detected by satellite observations (e.g., Webster et al. 1999, Ueda and Matsumoto 2000) and simulated by an oceanic model (Murtugudde et al. 2000). Thus, the ocean waves have a positive impact on the initial development of the IODM.

The third major difference lies in the existence of the South Asian monsoon and its interaction with adjacent tropical oceans. A warm SSTA in the northwest IO may enhance the Indian monsoon intensity through increased moisture fluxes (Meehl 1997). An enhanced monsoon may further affect the equatorial IO through remote and local processes[2] (Chang and Li 2000, hereafter CL00). To investigate the possible impact of the IODM on the Indian monsoon, we conducted ten-ensemble atmospheric general circulation model (AGCM) experiments with the Max-Planck Institute for Meteorology ECHAM4 model in a T42L19 resolution. For each ensemble run a slightly different initial condition was used. The AGCM is

---

[1] A positive phase of the IODM denotes a positive (negative) SSTA in the western (eastern) Indian Ocean, according to Saji et al. (1999).

[2] The local impact is through enhanced cross-equatorial winds and thus surface evaporation along the coast of Africa and the remote impact is through the change of large-scale east-west circulation and thus SSTA in the western Pacific/maritime continent that further affects local Walker circulation over the Indian Ocean.

forced by observed SST fields in 1997 in the tropical IO (30S-30N, 40E-110E) and climatological SST fields elsewhere. The atmospheric response to the IODM was obtained by subtracting the ensemble mean fields from those of a control experiment in which the climatological SST fields were specified in global oceans. The numerical simulations indicate that the IODM tends to enhance the Indian monsoon rainfall, which is consistent with results from a different AGCM by Ashok et al. (2001).

Given that a positive phase of the IODM enhances the monsoon, a natural question is how the anomalous monsoon further feeds back to the IODM. We argue that a strong Indian monsoon may enhance the northward cross-equatorial wind along the coast of Africa, leading to a cold SSTA in the western IO through enhanced surface evaporation, ocean mixing and coastal upwelling. Meanwhile, the strengthened monsoon may enhance the large-scale east-west circulation and leads to a positive SSTA in the western Pacific/maritime continent (CL00). As a result, the local Walker cell over the IO is enhanced. The enhanced Walker cell favors a warm (cold) SSTA in the eastern (western) IO through induced anomalous downwelling (upwelling) and the change of the thermocline depth/subsurface temperature. Both processes damp the IODM. Therefore, in addition to the cloud-SST feedback, the monsoon exerts another type of negative feedback on the IODM.

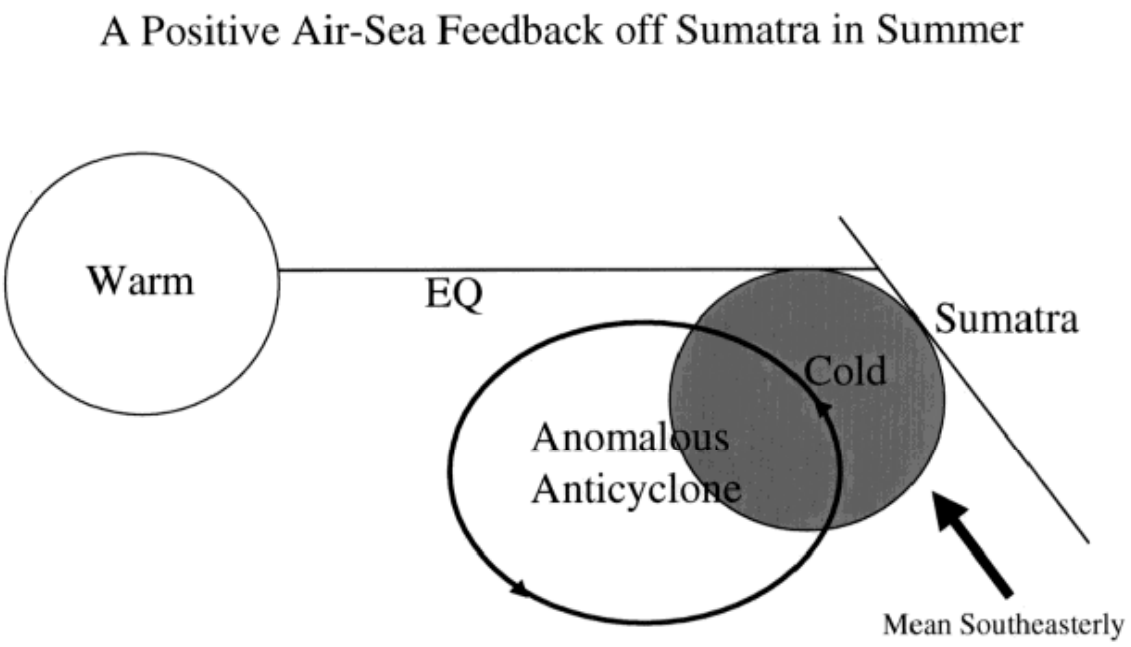

Fig. 5 Schematic diagram illustrating a positive thermodynamic air-sea feedback between an anomalous atmospheric anticyclone and a cold SSTA off Sumatra in the presence of boreal summer mean southeasterly flows.

The fourth difference is that the southeast IO is a region where there exists a positive atmosphere-ocean thermodynamic feedback (Wang et al. 2000). Compared to the southeast coasts of the tropical Pacific and Atlantic Oceans that are characterized by cold SST tongues and dense low-level stratus clouds, the southeast IO (off Sumatra) is a region with high mean SST and deep convection. The schematic diagram of Fig. 5 shows how a positive feedback between an anomalous atmospheric anticyclone and a cold SSTA works. Assume initially there is a modest cold SSTA off Sumatra. Since the southeast IO is a region of intense convection, the cold SSTA implies the decrease of atmospheric convective heating or an atmospheric heat sink. According to Gill's (1980) solution, the heat sink will induce a descending Rossby wave response to its west, resulting in anomalous low-level anticyclonic flows. In northern summer,

the mean flow is southeasterly. Thus the anomalous wind may enhance the total wind speed and lower the SST through enhanced surface evaporation, vertical mixing and coastal upwelling. Through this positive air-sea feedback, the cold SSTA and the anomalous anticyclone may develop (Wang et al. 2002).

Because of its dependence on the basic-state wind, the nature of this thermodynamic air-sea (hereafter, TAS) feedback is season-dependent. It is most efficient in boreal summer when the southeasterly flow is pronounced. With the seasonal change of the background flows from southeasterly in summer to northwesterly in winter, the same anomalous wind tends to reduce the total wind speed and thus damp the original cold SSTA. Thus, this mechanism acts as a negative feedback in northern winter. Because of its strong seasonal dependence, this TAS feedback mechanism may explain the rapid development of the IODM in boreal summer and its mature phase in October. The existence of the TAS feedback is consistent with the observational fact that the strongest IO SST variability appears off Sumatra.

3. A conceptual coupled model for the IODM

a) Governing equations

Our strategy is to construct the simplest model possible while considering essential air-sea feedback processes discussed in the previous section. For this purpose, we constructed a 5-box model illustrated in Fig. 6. Along the equator, the Indian Ocean is divided into two equal volume boxes, with T_{WI} and T_{EI} representing, respectively, the SSTA in the western IO (40°E-80°E) and eastern IO (80°E-120°E). To consider the monsoon-ocean interaction and the remote ENSO forcing, we consider additional 3 boxes. They represent, respectively, the South Asian monsoon region, the equatorial western Pacific/maritime continent (120°E-180°E), and the

eastern equatorial Pacific (180°E-80°W). The time change rate of the SSTA in the western equatorial IO may be written as

$$\frac{dT_{WI}}{dt} = -\lambda\Delta\overline{q}_{WI}\frac{\overline{V}_{WI}V_{WI}}{V_0} - (\lambda V_0\kappa + D_{SW})T_{WI} - u_I\overline{T}_I^{(x)} - \overline{u}_I T_I^{(x)} - w_{WI}\overline{T}_{WI}^{(z)} - \frac{\overline{w}_{WI}}{h}(T_{WI} - \gamma\eta_{WI}) \quad (1)$$

where the first two terms in the right side of (1) represent a linear form of surface wind-evaporation feedback, the third term the cloud-radiation-SST feedback, the fourth and fifth terms horizontal advection, and the last three terms the vertical temperature advection associated with anomalous upwelling and thermocline depth displacement. In (1), V, u, w, and η denote, respectively, the along-coastal wind, ocean zonal current, vertical velocity at the base of the oceanic mixed layer, and the thermocline depth; Δq denotes the air-sea specific humidity difference; γ represents the strength of subsurface ocean temperature variations associated with the thermocline displacement; $T^{(x)}$ and $T^{(z)}$ denote the zonal and vertical ocean temperature gradients; and h represents the depth of the mixed layer. Subscript *WI* stands for the western IO. An overbar represents the basic state field, and variables without the overbar represent anomalous fields. V_0 denotes a constant surface wind speed; κ an empirical constant relating SST and specific humidity; $\lambda = \rho_a c_D L/\rho c_w h$ where ρ and ρ_a are the density of water and surface air, c_w the specific heat of water, c_D the drag coefficient, and L the latent heat.

Similarly, the time change rates of the SSTA in the eastern equatorial IO and the western Pacific are governed by

$$\frac{dT_{EI}}{dt} = -\lambda\Delta\overline{q}_{EI}\frac{\overline{V}_{EI}V_{EI}}{V_0} - (\lambda V_0\kappa + D_{SW})T_{EI} - \overline{u}_I T_I^{(x)} - u_I\overline{T}_I^{(x)} - w_{EI}\overline{T}_{EI}^{(z)} - \frac{\overline{w}_{EI}}{h}(T_{EI} - \gamma\eta_{EI}) \quad (2)$$

$$\frac{dT_{WP}}{dt} = -\lambda\Delta\overline{q}_{WP}\frac{\overline{U}_{WP}U_{WP}}{V_0} - (\lambda V_0\kappa + D_{SW})T_{WP} - u_{CP}\overline{T}^{(x)}_{CP} - \overline{u}_{CP}T^{(x)}_{CP} - w_{WP}\overline{T}^{(z)}_{WP} - \frac{\overline{w}_{WP}}{h}(T_{WP} - \gamma\eta_{WP}) \quad , \tag{3}$$

where subscripts *EI, WP* and *CP* denote the eastern IO, western and central equatorial Pacific, respectively; and *U* denotes the zonal wind component.

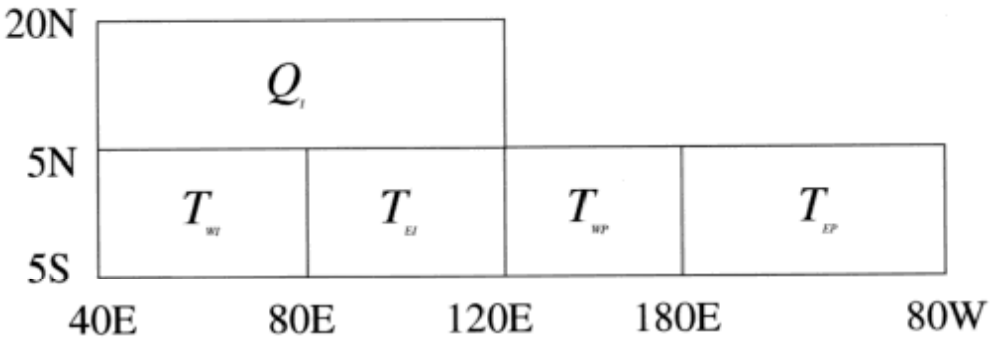

Fig. 6 Schematics of the five-box model. See text for details.

The change of the thermocline depth in the western and eastern IO depends on following two processes: 1) a fast response to the wind forcing so that the anomalous thermocline depth and zonal wind are approximately in a Sverdrup balance (Neelin 1991, Li 1997) and 2) a slow adjustment owing to the propagation of ocean waves (Schopf and Sureaz 1988):

$$\eta_{WI} = -\frac{\rho_a c_D V_0 L_I}{2g'\rho H}U_I(t) - c_0 U_I(t-\tau_1) \quad , \tag{4a}$$

$$\eta_{EI} = \frac{\rho_a c_D V_0 L_I}{2g'\rho H}U_I(t) - c_0 U_I(t-\tau_1-\tau_2) \quad , \tag{4b}$$

where *g'* is the reduced gravity, *H* the mean depth of the ocean thermocline, L_I the half width of the equatorial IO basin, $\alpha = \rho_a c_D V_0$, $\tau_1 = L_I / c_R$ and $\tau_2 = L_I / c_K$ represent, respectively, the traveling time of ocean Rossby waves from the central to western IO and of ocean Kelvin waves across the basin, and c_R and c_K denote the speed of equatorial oceanic Rossby and

Kelvin waves. Parameter c_0 represents the strength of the thermocline depth anomaly in response to unit wind forcing.

The thermocline depth anomaly in the western Pacific depends on the zonal wind anomaly in the central Pacific, that is,

$$\eta_{WP} = -\frac{L_P \alpha U_{CP}}{2\rho g' H} \tag{4c}$$

where L_P is the half width of the equatorial Pacific basin.

The anomalous monsoon heating over the South Asia depends on both local and remote processes. For the local processes, the heating anomaly is determined by anomalous moisture convergence in the atmospheric boundary layer (CL00, Li et al. 2001b), which can be parameterized as

$$Q_I^{(1)} = \delta_I b \rho_a \Delta z L(\nabla \cdot \vec{V} q)_I = \delta_I \sigma T_{WI} \ , \tag{5a}$$

where subscript I denotes the Indian monsoon; δ_I represents the seasonality of the monsoon heating with δ_I=1 for JJA (June-July-August) and δ_I=0 otherwise, b=*0.9* is a fraction of the moisture convergence that condenses out and releases the latent heat following Kuo (1974), Δz=1500 m denotes the depth of the atmospheric planetary boundary layer, and $q = (0.972T - 8.92) \times 10^{-3}$ is the surface air specific humidity, which is a function of SST (T) according to an empirical analysis by Li and Wang (1994).

Observations show that a dry Indian monsoon is often associated with an El Nino condition in the Pacific (Webster et al. 1998). To mimic this remote ENSO forcing, we parameterize the anomalous monsoon heating to be oppositely proportional to the eastern Pacific SSTA. Thus, the total anomalous heating may be written as

$$Q_I = \delta_I \sigma (T_{WI} - c_1 T_{EP}) \quad , \tag{5b}$$

where c_1 is a parameter representing the relative role of the local and remote SSTA forcing on the Indian monsoon. Given that the ratio of observed SSTA amplitude between the tropical IO and eastern Pacific is about 1:4, $c_1 > 0.25$ means that the remote ENSO forcing dominates the local SSTA effect.

The anomalous monsoon may further feed back to the ocean through enhanced/reduced cross-equatorial winds off the coasts of Africa:

$$V_{WI} = c_2' Q_I = \delta_I c_2 (T_{WI} - c_1 T_{EP}) \ . \tag{6a}$$

In addition to the remote effect on the monsoon, the El Nino may exert a strong impact on convection over the maritime continent. The suppression of convection in the maritime continent may further lead to anomalous southeasterly flows off Sumatra as an atmospheric Rossby wave response. Combining both the ENSO forcing and the TAS feedback in situ, one may express the along-coastal wind anomaly off Sumatra as

$$V_{EI} = c_3 T_{EP} - c_4 T_{EI} \ . \tag{6b}$$

The anomalous zonal wind over the central IO depends on east-west SST gradients (Lindzen and Nigam 1987) and the intensity of the local Walker cell, which is controlled by the SSTA in the maritime continent (CL00):

$$U_I = \frac{A}{\varepsilon L_I}(T_{EI} - T_{WI}) + c_5 T_{WP} + \tilde{f}(t)\text{,} \tag{7a}$$

where A is a SST-gradient momentum forcing coefficient (Wang and Li 1993) and ε is an atmospheric Rayleigh friction coefficient. The third term in the right hand side of Eq. (7a) represents the atmospheric ISO forcing over the equatorial IO. The inclusion of this term is to examine the role of the ISO on SST variability in the IO.

The anomalous zonal wind in the western Pacific is determined by the anomalous monsoon heating which, by altering the planetary-scale east-west circulation, changes the surface wind in the western Pacific/maritime continent (Barnett et al. 1989, Meehl 1997):

$$U_{WP} = -c_6' Q_I = -\delta_I c_6 (T_{WI} - c_1 T_{EP}). \quad (7b)$$

The anomalous zonal wind in the central equatorial Pacific is driven by the east-west SST gradient:

$$U_{CP} = \frac{A}{\varepsilon L_P}(T_{EP} - T_{WP}) \cdot \quad (7c)$$

The wind anomalies in turn drive anomalous ocean surface current and ocean vertical overturning. A simple 1.5-layer Cane-Zebiak (Cane 1979, Zebiak and Cane 1987) model is adopted to calculate the ocean surface currents and the Ekman pumping velocity. They are

$$u_I = \frac{\alpha U_I}{\rho h r} \ , \quad (8)$$

$$w_{WI} = -\frac{2(H-h)u_I}{L_I} \ , \quad (9)$$

$$w_{EI} = \frac{2(H-h)u_I}{L_I} \ , \quad (10)$$

$$u_{CP} = \frac{\alpha U_{CP}}{\rho h r} \ , \quad (11)$$

$$w_{WP} = -\frac{(H-h)\beta\alpha U_{WP}}{\rho H r^2} + \frac{2(H-h)u_{CP}}{L_P} \ . \quad (12)$$

Here β denotes the planetary vorticity gradient, H is the mean depth of the ocean thermocline, and r is a friction coefficient in the oceanic Ekman layer. Table 1 lists standard parameter values in the model. Note that interactive coefficients c_0, $c_1 ... c_6$ are determined by either a

regression from observational data or a scale analysis shown in CL00. For instance, we set c_0 = *5* s based on the observed sea level height-wind relationship that a 30 m height anomaly corresponds to a zonal wind anomaly of 6 m/s (see Fig. 4 of Webster et al. 1999); c_5=4 $ms^{-1}K^{-1}$ means that a half degree SSTA in the maritime continent leads to a zonal wind anomaly of 2 m/s in the central equatorial IO, which was derived from a scale analysis (see CL00 in detail) and supported by observations.

b) Basic State, Model Physics, and External Forcing

Observations show that winds along the coasts of Sumatra and Somalia exhibit a strong annual cycle. In response to the wind forcing, the coastal upwelling also exhibits a clear annual variation, with maximum amplitude appearing in boreal summer. To mimic this observed feature, we specify the basic-state wind and ocean vertical velocity as follows:

$$\overline{V}_{WI} = \overline{V}_{EI} = \overline{V}_0 \cos[\frac{2\pi(i-7)}{12}] , \tag{13}$$

$$\overline{w}_{WI} = \overline{w}_{EI} = \max\{\overline{w}_C, \overline{w}_0 \cos[\frac{2\pi(i-7)}{12}]\} , \tag{14}$$

where $i=1,2,\ldots,12$ represents January, February, …, December, and $\overline{w}_C$ is a minimum vertical velocity representing the background vertical mixing due to wind stirring. Same as in CL00, a seasonally varying background zonal wind is specified in the maritime continent/western Pacific.

Basic-state zonal wind and east-west SST gradient exhibit a clear semiannual cycle along the equatorial IO (Ueda 2001). To mimic this observational feature, we specify the following basic-state ocean current and zonal temperature gradient in the IO:

$$\overline{u}_I = \overline{u}_0 \cos[\frac{2\pi(i-4)}{6}] , \tag{15}$$

$$\overline{T}_I^{(x)} = -\overline{T}_0^{(x)} \cos[\frac{2\pi(i-4)}{6}] . \tag{16}$$

Essential physics in the model involve various positive and negative air-sea feedback processes. The negative feedback processes include the cloud-radiation-SST feedback, the wind-evaporation feedback, and the monsoon-ocean feedback. The positive feedback processes include the thermocline-SST-wind feedback and the TAS feedback. Different from the ENSO dynamics, ocean waves have a positive impact on the initial development of the IODM.

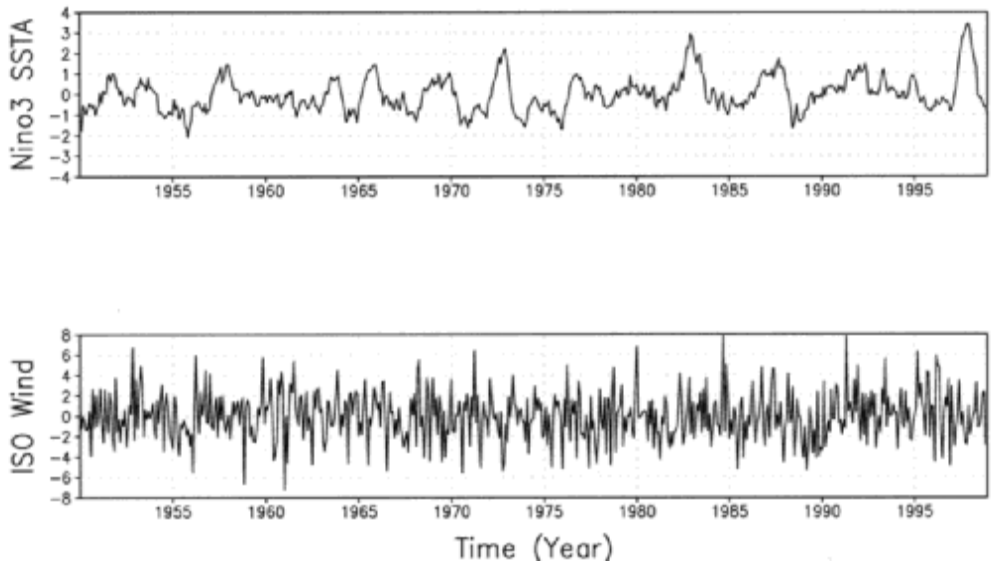

Fig. 7 Time series of the external ENSO and ISO forcing specified in the model. The top panel is the observed Nino 3 SSTA (°C) during 1950-1999. The bottom panel is the 10-90 day filtered zonal wind (ms^{-1}) in the central equatorial Indian Ocean (60-90E, 5S-5N).

In addition to the aforementioned feedback processes, the model is subjected to two types of external forcing, the ISO and ENSO. It has been noticed that the tropical IO is a region with strong intraseasonal variability. It is not clear, however, what role the ISO plays in interannual SST variability. As the greatest interannual variability in the tropics, ENSO may exert a strong impact on the IO (Chambers et al. 1999, Murtugudde et al. 2000). In the model, El Nino influences the IO through the following three processes: 1) cooling of the SSTA in the western Pacific/maritime continent, which further alters the strength of the local Walker cell over the IO, 2) decrease of intensity of the South Asian monsoon, which further reduces the strength of the Somalia Jet, and 3) suppression of convection in the maritime continent, which further induces anomalous southeasterly flow off Sumatra. To realistically describe the ISO and ENSO forcing, observed time series of the 10-90 day filtered zonal wind field in the central equatorial IO and the Nino3 SSTA during 1950-1998 were specified (see Fig. 7).

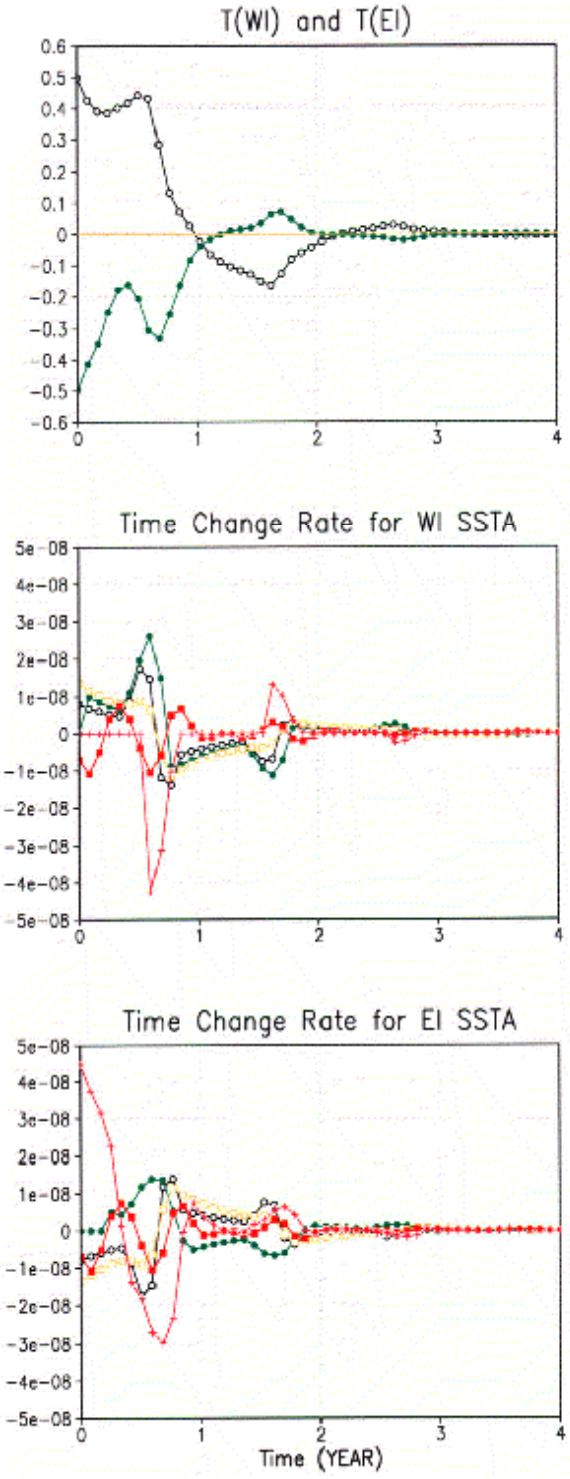

Fig. 8 Evolution of simulated SSTA (°C) in the western and eastern Indian Ocean in the absence of external forcing (top panel) and time tendencies of the SSTA (units: $^{o}Cs^{-1}$) in the western

(middle panel) and eastern (bottom panel) IO. The open and close circles denote anomalous vertical temperature advection associated with fast thermocline adjustments and slower oceanic wave effects. The open square represents the vertical temperature advection due to anomalous upwelling. The close square represents the horizontal temperature advection anomaly. The cross denotes the evaporation-SST-wind feedback associated with the anomalous monsoon for the western IO and the TAS feedback for the eastern IO.

4. IODM – A natural damped air-sea coupled mode

First we examine the model solutions in the presence of air-sea feedback processes mentioned above but without consideration of external forcing. Figure 8a shows the time evolution of the model SSTA in this case. Initially, a dipole SST structure, with $T_{WI} = 0.5^0 C$ and $T_{EI} = -0.5^0 C$, was specified. The numerical result indicates that ocean-atmosphere interactions in the IO support a damped oscillation mode, with a biennial periodicity.

Diagnosis of the surface heat budget indicates that the time change rate of T_{WI} is primarily determined by anomalous vertical temperature advection (including the effect of ocean waves) and evaporational cooling associated with the monsoon-ocean local feedback (Fig. 8b). The time change rate of T_{EI} is strongly regulated by the seasonal-dependent TAS feedback (Fig. 8c). The anomalous vertical temperature advection tends to enhance T_{EI} in the initial development stage due to the positive thermocline-SST feedback, but tends to decrease T_{EI} later owing to the delayed effect of the ocean waves. In both regions, the cloud-radiation-SST feedback contributes greatly to damping the SSTA, while the zonal advection anomaly has modest amplitude with a semiannual periodicity.

The sensitivity tests with different parameter values (say, 20% increase or decrease of the interactive coefficients c_0, $c_1 ... c_6$) indicate that the damped oscillation solution is quite

robust. This indicates that the IODM is a natural damped air-sea coupled mode. The greatest negative feedback comes from the cloud-radiation-SST feedback. As discussed in the previous sections, this strong negative feedback is active only in the warm oceans; therefore it does not significantly damp El Nino. The additional negative feedback results from the monsoon-ocean interaction. While a positive phase of the IODM strengthens the monsoon, the enhanced monsoon tends to damp the dipole through both remote and local processes. The ocean waves contribute positively to the growth of the SSTA in the western IO, but their impact is much weaker compared to El Nino scenario because the mean thermocline in the eastern Pacific is much shallower. The TAS feedback is a positive feedback mechanism in the southeast IO, but because of its seasonal dependence it is only effective in boreal summer. In boreal winter it acts as a strong damping. The net effect of these feedback processes results in a damped oscillation mode in the tropical IO, which is different from the self-sustained ENSO mode in the Pacific. The fundamental difference arises from the distinctive characteristics of the basic state of the coupled system in the two oceans.

5. Role of external forcing

To examine the impact of the ISO, we designed a set of numerical experiments in which the strength of the ISO was gradually increased to 25%, 50%, and 100% of the observed amplitude. Figure 9 shows the SSTA evolution in the three cases. With enhanced ISO variability, the naturally damped SST mode tends to oscillate around a finite amplitude. The results suggest that the ISO may act as stochastic forcing to reinvigorate the natural damped mode. However, even with the full strength of the ISO forcing, the amplitude of the SSTA is still much smaller compared to the observed SSTA variability.

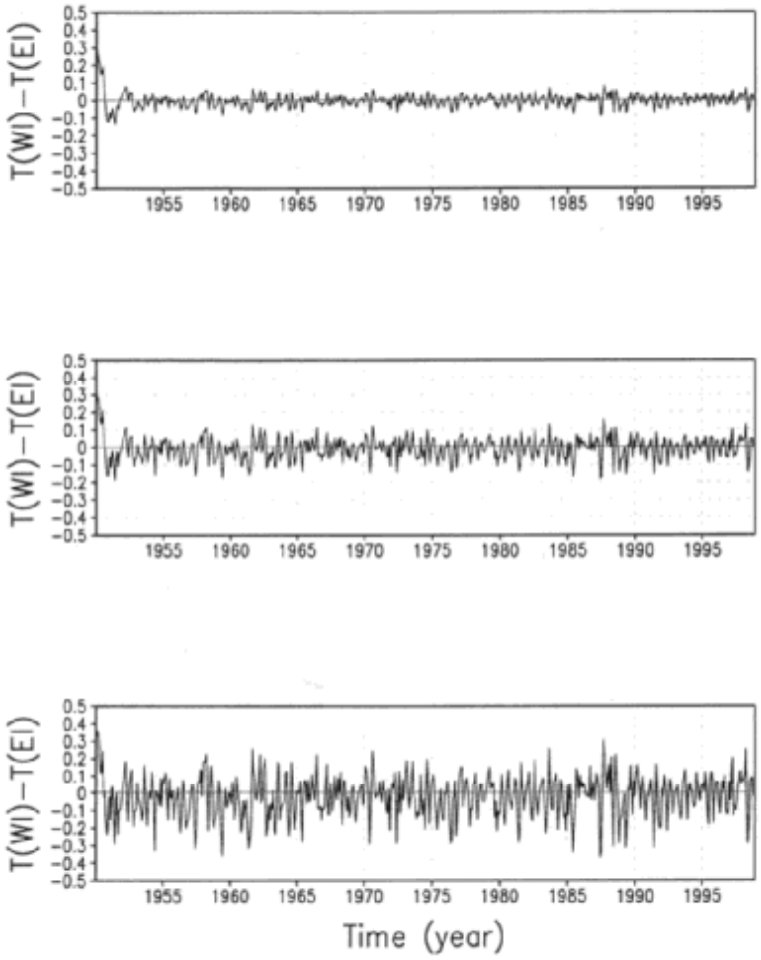

Fig. 9 Evolution of the SSTA difference (°C) between the western and eastern IO in the presence of a quarter (top panel), a half (middle panel), and full (bottom panel) strength of the observed ISO wind forcing in the central equatorial IO. All other parameters are same as those in Fig. 8.

In the presence of the realistic El Nino forcing, the model is capable of simulating several major IODM events (such as in 1997, 1972, 1982, and 1963) during last 50 years except in 1961 and 1994. (The special characteristics of the 1961 and 1994 events is discussed in section 9.) Figure 10 shows the model simulated SSTA in the western and eastern IO, along with observed counterparts. The model is capable of simulating the magnitude and phase of the

IODM events reasonably well. The results suggest that ENSO is one of the major forcing mechanisms that trigger the IODM events.

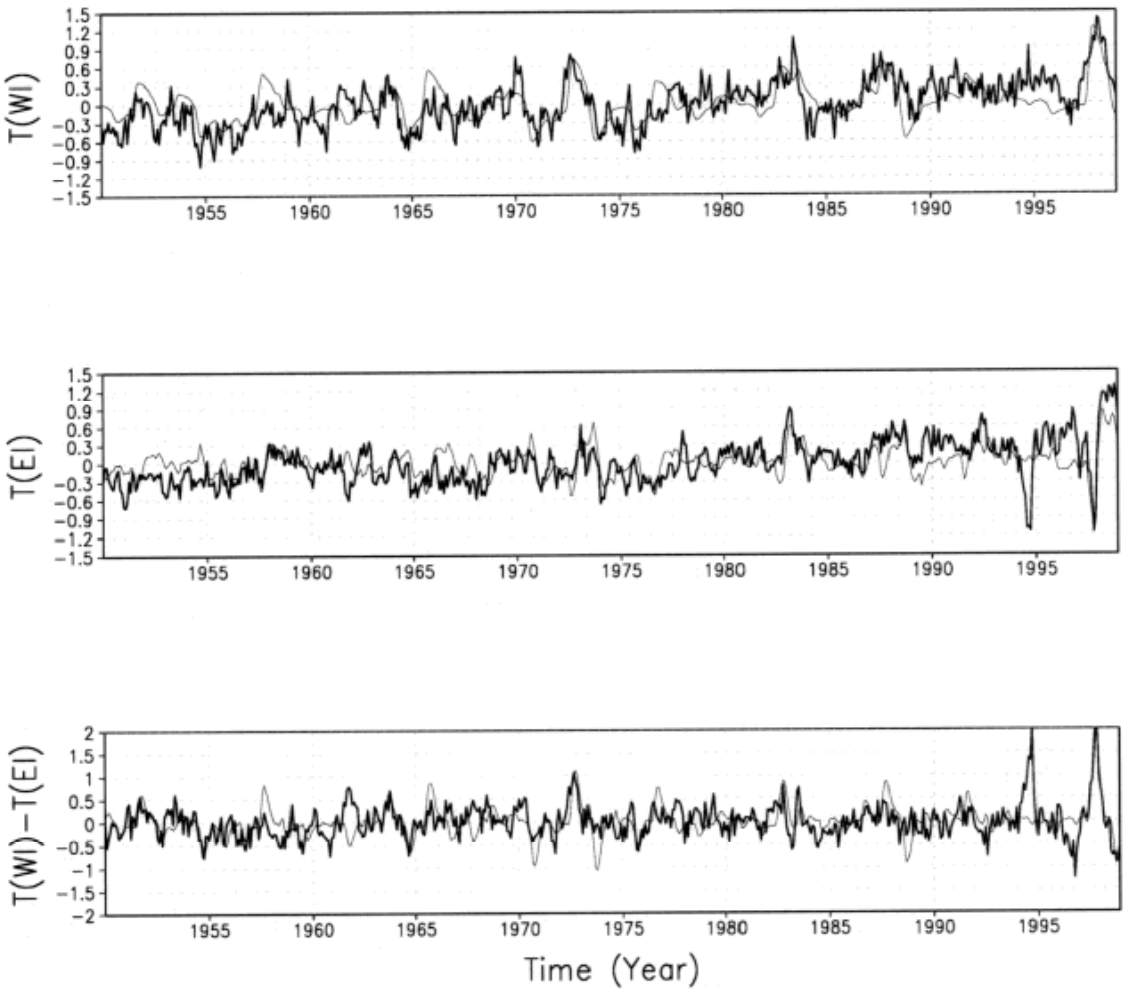

Fig. 10 Evolution of observed (thick line) and simulated (thin line) SST anomalies (°C) in the western (top panel) and eastern (middle panel) Indian Ocean and their differences (bottom panel). Observed El Nino and ISO forcing was specified in this case, and all other parameters have the same values as those in Fig. 8.

In the model the El Nino influences the IODM mainly through the change of intensity of the Indian monsoon and of convection/SST over the maritime continent. The former primarily impacts the western IO SSTA, whereas the latter primarily influences the eastern IO.

To investigate their relative roles, two additional experiments were conducted in which we separated the two processes. It turns out that both processes contribute nearly equally to the development of the IODM (figure not shown).

6. Phase-locking mechanism

Although the El Nino has a great influence on the IO, it is the ocean-atmosphere interactions in situ that regulate the life cycle of the IODM. This is why the mature phase of the IODM occurs in October even though the maximum ENSO forcing appears in northern winter. There are several possible factors that may cause the phase locking of the IODM. The first is the annual cycle of the basic-state wind off Sumatra. This seasonally varying basic-state wind regulates the local SST change through the TAS feedback mechanism. In addition, the seasonal change of mean upwelling off the coasts of Sumatra and Somalia may also play a role. This is because even given the same thermocline depth anomaly, the seasonally varying mean upwelling may lead to the greatest SST tendency in boreal summer when the upwelling is strongest. The third possible factor is the annual cycle of east-west SST gradients and zonal winds along the equator. Ueda (2001) suggested that the sum of basic-state and anomalous SST might give rise to maximum amplitude in northern fall. The fourth factor is the seasonal dependence of the anomalous monsoon heating. Although the El Nino exerts the strongest forcing toward the end of a year, its impact on anomalous monsoon heating peaks in northern summer. Thus the anomalous monsoon may exert the greatest impact on the IO toward the end of summer.

Figure 11 shows the composite time evolution of the Dipole Mode Index (DMI, defined as the SSTA difference between the western and eastern IO) and zonal wind anomaly

in the central equatorial IO. The composite is based on seven strongest IODM events simulated in Fig. 10. Note that the mature phase of the model IODM occurs in October, and the phases of the IODM in the model well lock into the annual cycle.

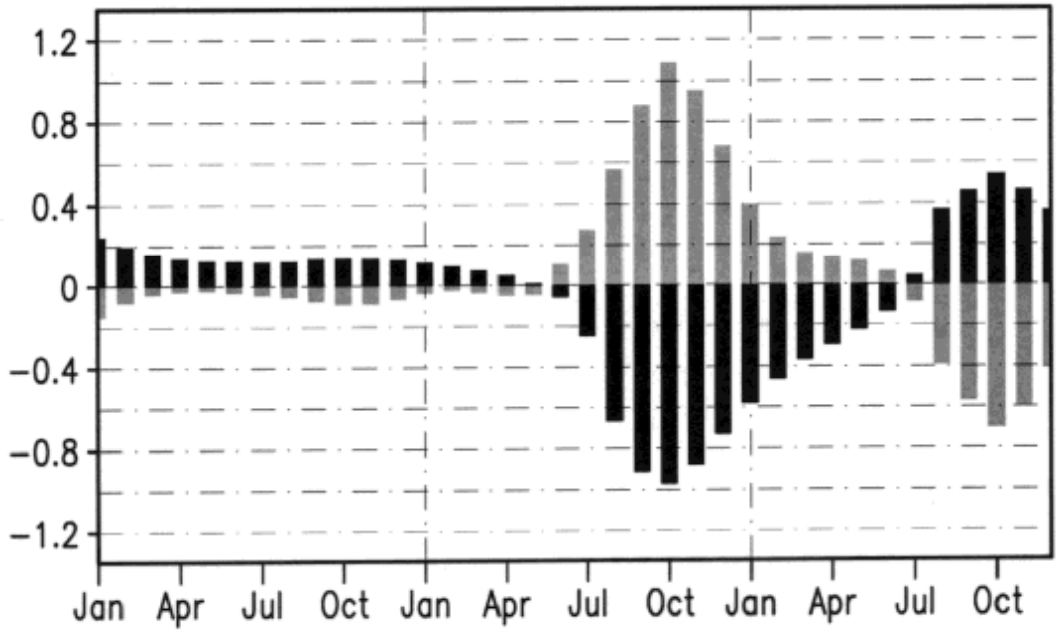

Fig. 11 Evolution of the model composite SSTA difference (°C, light shaded bar) and zonal wind anomaly (units: 2 ms^{-1}, dark shaded bar) in the Indian Ocean.

To investigate the relative roles of the aforementioned factors, we designed the following four experiments. In the first experiment, we considered the annual cycle of $\overline{V}_{EI}$ while other basic-state variables were set to their annual mean values. In the second experiment, we considered the seasonally varying $\overline{w}_{EI}$ and $\overline{w}_{WI}$ only. In the third experiment the effect of annual cycle of $\overline{u}_I$ and $\overline{T}_I^{(x)}$ was examined. In the fourth experiment we considered the seasonally varying $\overline{V}_{WI}$ and $\overline{U}_{WP}$.

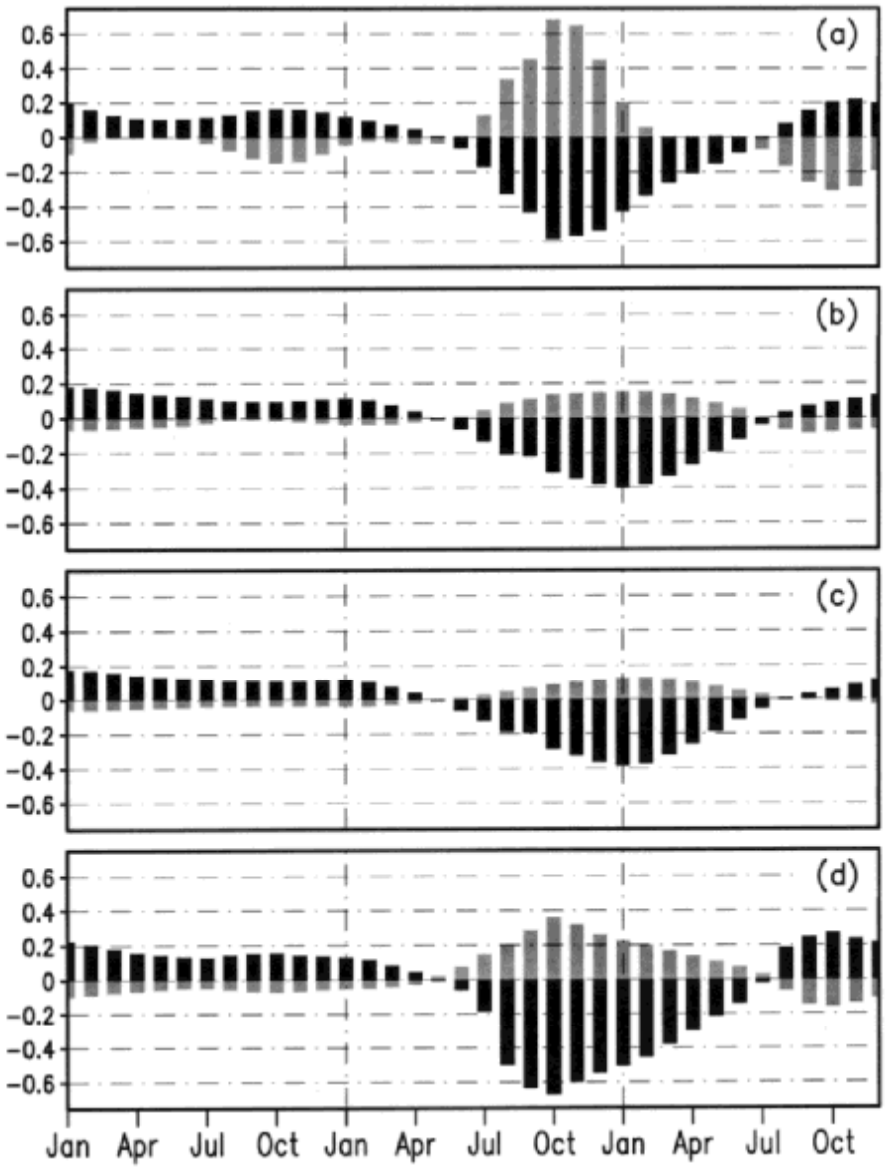

Fig. 12 Same as Fig. 11 except for specification of different annual cycle basic states. The top panel is a case when only the annual cycle of the wind over the eastern IO is included. The panel below shows a case in which only the annual cycle of ocean upwelling along the coasts of Africa and Sumatra is considered. The next panel shows a case of annually varying zonal oceanic currents and zonal temperature gradients. The bottom panel is a case that considers the annual cycle of the wind in both the western IO and the maritime continent.

Figure 12 shows the results from the four experiments. Note that in experiments 1 and 4 the mature phases of the IODM appear in October, whereas in experiments 2 and 3 they

appear in January. The results indicate that the primary mechanisms for the phase locking arise from the seasonal-dependent TAS feedback (Fig. 12a) and the remote and local impact of the anomalous monsoon (Fig. 12d). The effect of the seasonal varying basic-state upwelling and zonal temperature gradient is small (Figs. 12b and c).

7. Effect of ocean waves

The time evolution of the observed SSTA in 1997 shows that the SST dipole developed rapidly in summer and reached its mature phase in fall 1997. After that, the cold SSTA in the eastern IO started to decay, and the warm SSTA in the western IO spread into the east. By the middle of the 1997/98 winter, a basin-wide warming (hereafter, a unimode) was observed.

Such a dipole-to-unimode transition is well captured by the model. Figure 13a illustrates the time evolution of the model simulated SSTA in 1997, along with observed counterparts. Similar to the observations, after the cold SSTA reached its maximum amplitude in October in the eastern IO, it decayed rapidly and became positive in December 1997. What causes such a dipole-to-unimode transition? The diagnosis of the SSTA budget showed that the primary mechanism for this SSTA transition was attributed to the delayed effect of the ocean waves. In response to anomalous zonal SST gradients, easterly wind anomalies were generated in the central equatorial IO. The curl of the anomalous easterlies excited equatorial Rossby waves that carried positive thermocline depth anomaly signals and propagated westward. After reflection from the western boundary, they became downwelling equatorial Kelvin waves and propagated eastward. The eastward expansion of the warm SSTA was attributed to the

accumulated effect of these oceanic waves. When the wave effect is excluded (by setting c_0 =0), the SSTA transition does not occur (see Fig. 13b).

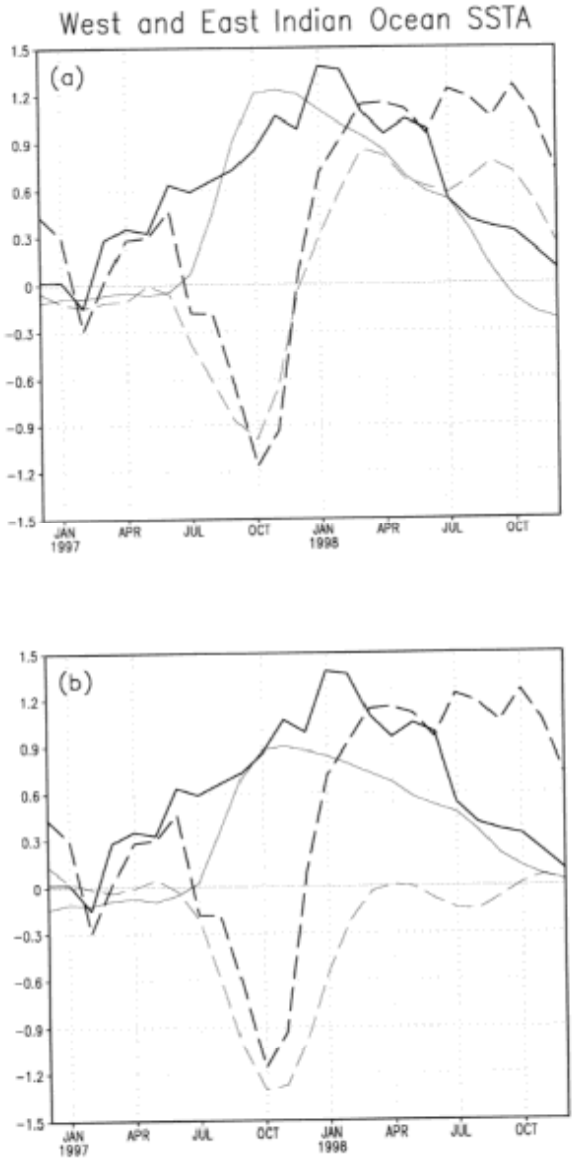

Fig. 13 Evolution of the observed (thick line) and simulated (thin line) SSTA (°C) in the western (solid line) and eastern (dashed line) IO associated with the 1997-98 IODM event. The top panel is the case that includes the effect of oceanic waves and the bottom panel is a case without the oceanic wave effect.

8. Biennial tendency of the IODM

The composite SST and wind evolution (Fig. 11) shows that the model IODM has a biennial tendency, similar to the observation. What cause this biennial tendency? One obvious factor is the ENSO forcing, because the Nino3 SSTA has a power-spectrum peak on the quasi-biennial frequency. Another possible factor is the monsoon-ocean interaction. Li et al. (2001a) pointed out that this interaction is essential for the tropospheric biennial oscillation in the Asian-Australian monsoon region. To illustrate the role of the monsoon, we conducted an experiment in which all parameters were same as those in Fig. 8a except that we turned off the monsoon effect (by simply setting $Q_I = 0$). The result clearly illustrates the role of the monsoon-ocean feedback in causing the biennial tendency of the IODM. Contrary to the case in Fig. 8a in which the SSTA in both the eastern and western IO change the sign from one year to the following year, the SSTA does not cross the zero line in the case with no monsoon-ocean feedback (Fig. 14).

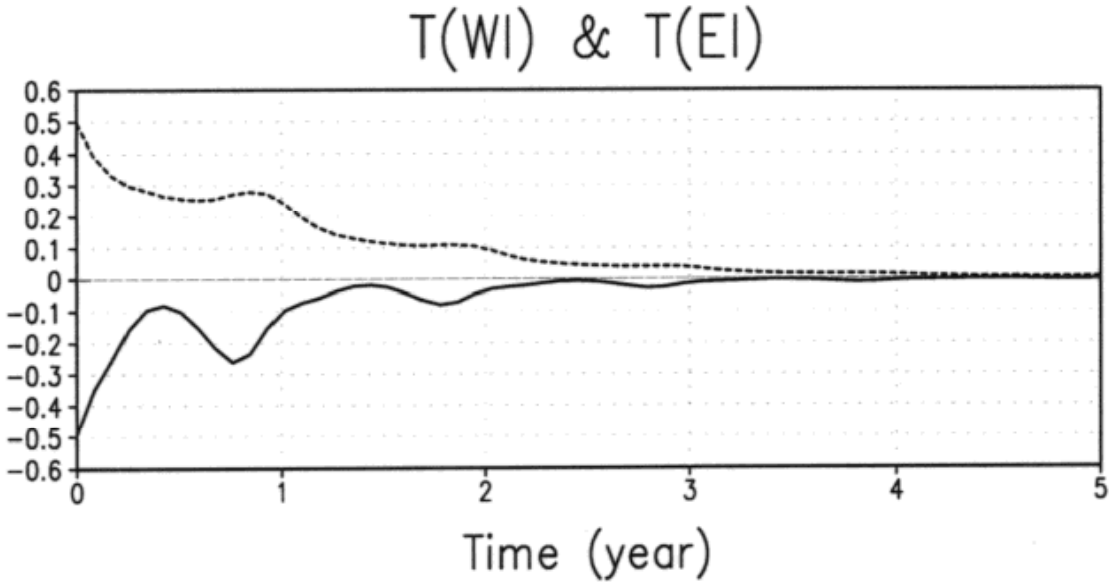

Fig. 14 Evolution of the SSTA (°C) in the western (dashed line) and eastern (solid line) IO in the absence of the monsoon feedback. All other parameters are same as those in the case shown in

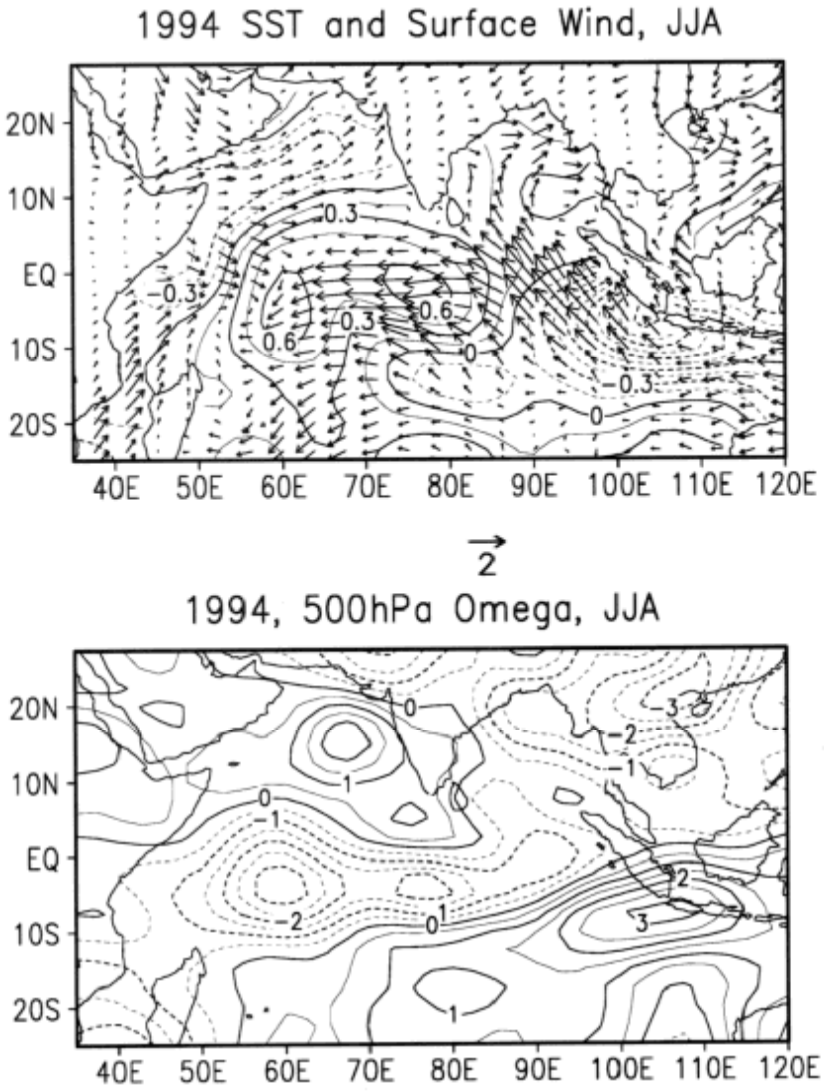

Fig. 15 Horizontal patterns of SST (°C) and surface wind (ms^{-1}) anomalies (top panel) and anomalous 500 hPa vertical velocity field (units: $10^{-2} Pas^{-1}$, bottom panel) in JJA of 1994

How does the monsoon-ocean feedback lead to a biennial tendency? As we know, a positive phase of the IODM may lead to a strong Indian monsoon. The enhanced monsoon induces anomalous east-west circulation, leading to a positive tendency of the SSTA in the maritime continent (CL00). The anomalous warming in the maritime continent further exerts a delayed impact on the equatorial IO through the enhanced local Walker cell, leading to a negative phase of the IODM. Thus it is the lagged response of the maritime continent SSTA to the anomalous monsoon that gives rise to the biennial tendency.

9. IODM events in 1994 and 1961

The occurrences of the IODM events in 1994 and 1961 suggest that the SST variability in the IO cannot be simply explained by the ENSO forcing. Other types of climate forcing may also play a role in initiating/triggering the coupled modes over the tropical IO. The question is what triggered the IODM events in 1994 and 1961.

Figure 15 illustrates the 1994 summer SSTA and 500 hPa vertical motion anomaly derived from the NCAR/NCEP reanalysis. (The middle tropospheric vertical motion is used to represent atmospheric convective heating in the tropics.) It is noted that the development of the 1994 IODM event started from the eastern IO where a cold SSTA was initiated in early summer in response to enhanced southeasterly flows along the Sumatra coast. The anomalous northward cross-equatorial flows in the eastern IO resulted from anomalous atmospheric heating over Indochina/South China Sea, which persisted from late spring (May) through summer. Therefore, we conclude that the 1994 IODM event was initiated by anomalous heating over Indochina/South China Sea. This anomalous heat source was not related to El Nino, because the eastern Pacific SSTA was in a normal condition.

Unlike many IODM events that were initiated in early summer, the 1961 event may be traced back to DJF of 1960-61 when a modest cold SSTA developed in the eastern IO (left panels of Fig. 16). It is likely that this cold SSTA resulted from enhanced westerly (and thus surface evaporation) at the equator in response to anomalous heating in the maritime continent, which is represented by anomalous vertical motion at 500 hPa (right panels of Fig. 16). Meanwhile a weak warming developed in the western equatorial IO off the coast of Africa, due to warm SST advection from the southern IO (around 10-15°S) in boreal winter. This enhanced the zonal SST gradient along the equator. The enhanced zonal SST gradient tended to

manifest itself in a way that it overcame natural dissipations and maintained the dipole structure throughout spring. After summer arrived, the TAS feedback and the thermocline-SST feedback tended to enhance the dipole so that it developed rapidly.

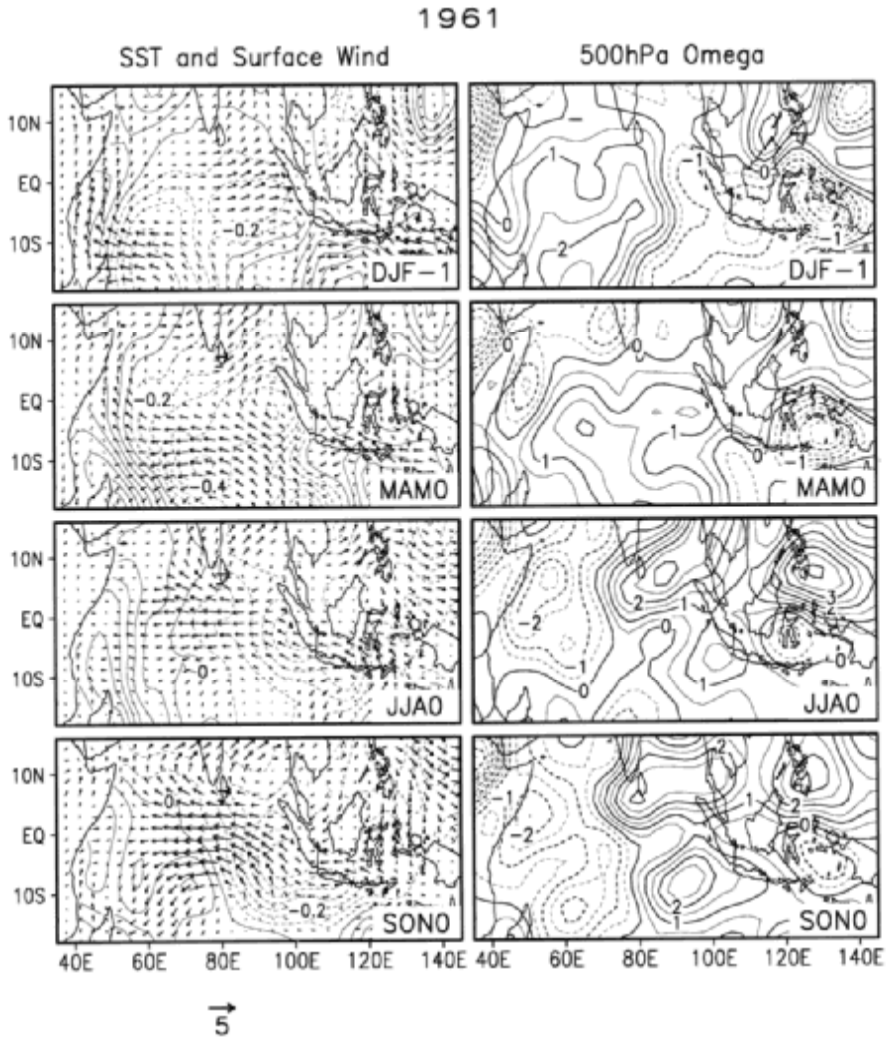

Fig. 16 Evolution of the 1961 IODM event from the preceding winter to the peak phase. The left panels show SST (°C) and surface wind (ms^{-1}) anomalies, and the right panels show 500 hPa vertical velocity anomalies (units: $10^{-2} Pas^{-1}$).

10. Concluding remarks

A conceptual coupled atmosphere-ocean model was constructed to understand the origin of the Indian Ocean Dipole Mode (IODM). This model contained 5 boxes that represent the equatorial western and eastern Indian Ocean, the western Pacific/Maritime Continent, the equatorial eastern Pacific, and the South Asian monsoon region, respectively. In the model, various positive and negative feedback processes attribute to the Indian Ocean SST variability. Among them are the cloud-radiation-SST feedback, evaporation-SST-wind feedback, thermocline-SST feedback, and the monsoon-ocean interaction. We addressed the following scientific questions: What are fundamental differences between air-sea interactions in the tropical Pacific and those of the Indian Ocean? Why does the peak phase of the IODM appear in October? What are physical mechanisms responsible for the biennial tendency of the IODM? Is the IODM a damped or self-sustained air-sea coupled mode? What roles do the ENSO and ISO play in the IODM evolution?

Our results indicate that air-sea interactions in the Indian Ocean in general support a natural damped mode, which is different from the self-sustained ENSO mode in the Pacific. The difference arises primarily from the distinctive characteristics of the basic state of the coupled system in the tropical Indian and Pacific Oceans. There are four major differences between air-sea coupling processes in the two oceans. The first difference is represented by the strong contrast of the cloud-SST phase relationship between the warm pool and cool tongue. Because of the in-phase cloud-SST relationship in warm oceans, the SST variability is greatly suppressed. The second difference arises from the reversal of the basic-state zonal wind and east-west tilting of the ocean thermocline, which leads to distinctive effects of ocean waves on the SST. The third difference lies in the existence of the Asian monsoon and its interaction

with the adjacent oceans. The fourth difference is that the southeast Indian Ocean is a region where there exists a positive thermodynamic air-sea feedback. Because of these differences, air-sea interactions tend to support a damped oscillation mode in the IO but a self-sustained oscillation mode in the Pacific. The strongest damping comes from the shortwave radiation-cloud-SST feedback. The monsoon also exerts a negative impact on the IODM.

Contrary to the southeast tropical Pacific and Atlantic oceans characterized by cold SST tongues and dense low-level stratus clouds, the southeast IO (off Sumatra) is a region with high mean SST and deep convection. Because of this distinctive feature, a positive thermodynamic air-sea feedback exists in the southeast Indian Ocean. This positive feedback arises from interactions between an anomalous atmospheric anticyclone and a cold SSTA, and is season-dependent due to its dependence on the basic state wind. The positive feedback is most efficient in boreal summer when the southeasterly flow is pronounced. The phase locking feature of the IODM can be, to a certain extent, explained by the seasonal dependence of this thermodynamic feedback mechanism. In addition, the anomalous monsoon also plays a role. Although the El Nino has the greatest amplitude toward the end of a year, its impact on the anomalous monsoon heating peaks in northern summer. Therefore, the anomalous monsoon may exert the strongest impact on the IODM toward the end of summer. Our sensitivity experiments indicate that the phase-locking of the IODM is primarily caused by the two factors.

Different from the ENSO dynamics, ocean waves have a positive impact on the initial development of the IODM. A transition from a dipole to an unimode is mainly attributed to ocean waves through their accumulated effects on the thermocline and subsurface temperature

changes. The biennial tendency of the IODM arises from the external forcing of ENSO and the monsoon-ocean feedback.

The role of the ISO was investigated by forcing the model with the observed ISO wind in the central equatorial Indian Ocean. With the increase of strength of the ISO forcing, the model simulates a sustained, irregular oscillation, suggesting that the ISO may act as a stochastic forcing to reinvigorate the naturally damped IODM.

While the ISO primarily represents atmospheric stochastic forcing, the ENSO has a more profound impact on the IODM, due to its long duration and great amplitude. In the model an El Nino impacts the IODM through the following three processes. First, it influences the strength of the South Asian monsoon, which further alters the cross-equatorial wind along the coast of Africa. Second, it altered the anomalous Walker cell over the IO through the change of SST in the maritime continent/western Pacific. Third, it influences the intensity of convection over the maritime continent, which further induces anomalous along-coastal winds off Sumatra. All three processes favor the initiation and development of a positive phase of the IODM.

In the presence of realistic ENSO forcing, the model was capable of simulating several IODM events during recent 50 years that were associated with the ENSO. However, it failed to simulate the IODM events in 1961 and 1994. Further observational analyses indicated that the IODM events in 1961 and 1994 have special characteristics. The 1994 event was initiated by anomalous heating over Indochina/South China Sea in late spring/early summer. In response to this anomalous heating, northward cross-equatorial flows were established. The anomalous along-coastal wind off Sumatra causes the cooling in situ, which initiated the dipole event. The 1961 event was initiated by anomalous heating over the maritime continent in northern winter.

In response to the anomalous heating, a weak SST dipole was established. This zonal SST gradient tended to manifest itself in a way that it overcame natural dissipations and maintained the dipole structure throughout spring. After summer arrived, it developed rapidly, owing to the thermodynamic air-sea feedback and the wind-thermocline-SST feedback. Given the observational fact that both the IODM events were independent of the ENSO, it is conceivable that other types of climate forcing in addition to ENSO may trigger/initiate an IODM event.

Acknowledgments. This work was supported by the NOAA Grant NA01AANRG0011, by NSF Grant ATM01-19490, and by the International Pacific Research Center that is partially sponsored by the Frontier Research System for Global Change. This is SOEST contribution number xxxx and IPRC contribution number xx.

References

Ashok, K., Z. Guan, and T. Yamagata, 2001: Impact of the Indian Ocean dipole on the relationship between the Indian monsoon rainfall and ENSO. *Geophy. Res. Lett*., in press.

Battisti, D. S., and A.C. Hirst, 1989: Interannual variability in the tropical atmosphere-ocean system: Influence of the basic state and ocean geometry. *J.Atmos.Sci*., **46**, 1678-1712.

Barnett, T. P., L. Dumenil, U. Schlese, E. Roeckner, and M. Latif, 1989: The effect of Eurasian snow cover on regional and global climate variations. *J. Atmos. Sci.*, **46**, 661-685.

Cane, M. A., 1979: The response of an equatorial ocean to simple wind stress patterns. I: Model formulation and analytic results. *J. Mar. Res.*, **37**, 233-252.

Chambers, D.P., B.D. Tapley, and R.H. Stewart, 1999: Anomalous warming in the Indian Ocean coincident with El Nino. *J.Geophys.Res*., **104**, 10523-10533.

Chang, C.-P., and T. Li, 2000: A theory for the tropical tropospheric biennial oscillation. *J. Atmos. Sci*, **57**, 2209-2224.

Gill, A. E., 1980: Some simple solutions for heat-induced tropical circulation. *Quart. J. Roy. Meteor. Soc.*, **106**, 447-462.

Kuo 1974 Kuo, H.-L., 1974: Further studies of the parameterization of the influence of cumulus convection on large-scale flow. *J. Atmos. Sci.*, **31**, 1231-1240.

Li, T., 1997: Phase transition of the El Nino-Southern Oscillation: A stationary SST mode. *J. Atmos. Sci*., **54**, 2872-2887.

_____, C.-W. Tham, and C.-P. Chang, 2001a: A coupled air-sea-monsoon oscillator for the tropospheric biennial oscillation. *J. Climate*, **14**, 752-764.

_____, Y.S. Zhang, C.P. Chang, B. Wang, 2001b: On the relationship between Indian Ocean SST and Asian summer monsoon. *Geophy. Res. Let*., **28**, 2843-2846.

_____, and B. Wang, 1994: A thermodynamic equilibrium climate model for monthly mean surface winds and precipitation over the tropical Pacific. *J. Atmos. Sci.*, **51**, 1372-1385.

Lindzen, R. S., and S. Nigam, 1987: On the role of sea surface temperature gradients in forcing low level winds and convergence in the tropics. *J. Atmos. Sci*., **44**, 2240-2458.

Meehl, G. A., 1997: The south Asian monsoon and the tropospheric biennial oscillation. *J. Climate*, **10**, 1921-1943.

Murtugudde, R., J.P. McCreary Jr, A.J. Busalacchi, 2000: Oceanic processes associated with anomalous events in the Indian Ocean with relevance to 1997-1998. *J. Geophy. Res*., **105**, 3295-3306.

Neelin, J.D., 1991: The slow sea surface temperature mode and the fast wave limit: Analytical theory for tropical interannual oscillation and experiments in a hybrid coupled model. *J.Atmos.Sci*., **48**, 584-606.

Reverdin, G., D.L. Cadet, and D. Gutzler, 1986: Interannual displacement of convection and surface circulation over the equatorial Indian Ocean. *Quart.J.Roy.Met.Soc*., **112**, 43-67.

Saji, N.H., B.N. Goswami, P.N. Vinayachandran, and T. Yamagata, 1999: A dipole mode in the tropical Indian Ocean. *Nature*, **401**, 360-363.

Schopf, P.S., and M.J. Suarez, 1988: Vacillations in a coupled ocean-atmosphere model. *J.Atmos.Sci*., **45**, 549-566.

Ueda, H., 2001: Equatorial monsoon system as regulation for a dipole mode in the Indian Ocean. *Papers in Meteorology and Geophysics*, Vol. **51**, 147-154.

_____, and J. Matsumoto, 2000: A possible process of east-west asymmetric anomalies over the Indian Ocean in relation to 1997/98 El Nino. *J.Meteor.Soc.Japan*, Vol. **78**, 803-818.

Wang, B. and T. Li, 1993: A simple tropical atmospheric model of relevance to short-term climate variations. *J. Atmos. Sci*., **50**, 260-284.

_____, R. Wu, and X. Fu, 2000: Pacific-East Asian teleconnection: How does ENSO affect East Asian climate? *J. Climate*, **13**, 1517-1536.

_____, _____, and T. Li, 2002: Coupled monsoon-ocean modes and Asian-Australian monsoon variability. Submitted to J.*Climate*.

_____, and X. Xie,1998: Coupled modes of the warm pool climate system. Part I: The role of air-sea interaction in maintaining Madden-Julian Oscillation. *J.Climate*, **11**, 2116-2135.

Webster, P. J., V. O. Magana, T. N. Palmer, J. Shukla, R. A. Tomas, M. Yanai, and T. Yasunari, 1998: Monsoons: Processes, predictability, and the prospects for prediction. *J. Geophys. Res.*, **103-C7**, 14451-14510.

_____, A.M. Moore, J.P. Loschnigg, and R.R. Leben, 1999: Coupled ocean-atmosphere dynamics in the Indian Ocean during 1997-98. *Nature*, **401**, 356-360.

Xie, S.-P., H. Annamalai, F.A. Schott, J.P. McCreary, Jr., 2002: Structure and mechanisms of South Indian Ocean climate variability. *J.Climate*, 864-878.

Zebiak, S.E., and M.A. Cane, 1987: A model ENSO. *Mon. Wea. Rev*., **115**, 2262-2278.

Table 1. List of values of model parameters

ρ_a	1.2 $kg\ m^{-3}$	$\overline{T}_0^{(x)}$	$4x10^{-7}\ K\ m^{-1}$
c_D	1.5×10^{-3}	$\overline{u}_0$	0.1 ms^{-1}
V_o	5 ms^{-1}	$\overline{V}_0$	4 ms^{-1}
h	50 m	$\overline{U}_{wp}$ n. summer	2 ms^{-1}
H	150 m	$\overline{U}_{wp}$ n. winter	-2 ms^{-1}
$g' = \frac{c_s^2}{H}$	$\frac{2.5^2}{150} ms^{-2}$	$\overline{T}_{wl}^{(z)}, \overline{T}_{El}^{(z)}$	0.02 $K\ m^{-1}$
A	50 $m^2 s^{-2} K^{-1}$	$\overline{T}_{wp}^{(z)}$	0.01 $K\ m^{-1}$
ε	$10^{-5}\ s^{-1}$	$\overline{W}_0$	$4x10^{-6}\ ms^{-1}$
L_l	$4x10^6\ m$	$\overline{w}_c$	$10^{-6}\ ms^{-1}$
L_p	$8x10^6\ m$	$\Delta\overline{q_{wl}}, \Delta\overline{q_{El}}, \Delta\overline{q_{wp}}$	$5x10^{-3}$
γ	0.1 $K\ m^{-1}$	r	$10^{-5}\ s^{-1}$
κ	$7x10^{-4}\ K^{-1}$	c_0	5 s
c_1	0.4	c_2	1 $ms^{-1} K^{-1}$
c_3	0.5 $ms^{-1} K^{-1}$	c_4	1 $ms^{-1} K^{-1}$
c_5	4 $ms^{-1} K^{-1}$	c_6	2 $ms^{-1} K^{-1}$